

# Syntheses, characterizations and crystal structures of two lead(II) phosphonate–sulfonate hybrid materials

Jun-Ling Song, Chong Lei, Yan-Qiong Sun, and Jiang-Gao Mao\*

State Key Laboratory of Structure Chemistry, Fujian Institute for Research on the Structure of Matter, The Chinese Academy of Sciences, Fuzhou, Fujian 350002, People's Republic of China

Received 17 January 2004; received in revised form 23 March 2004; accepted 28 March 2004

## Abstract

Hydrothermal reactions of lead(II) acetate with 5-sulfoisophthalic acid monosodium salt ( $\text{NaH}_2\text{BTS}$ ) and *N*-(phosphonomethyl)-*N*-methylglycine,  $\text{MeN}(\text{CH}_2\text{CO}_2\text{H})(\text{CH}_2\text{PO}_3\text{H}_2)$  ( $\text{H}_3\text{L}^1$ ), or a new aminodiphosphonic acid, 3-Pyridyl- $\text{CH}_2\text{N}(\text{CH}_2\text{PO}_3\text{H}_2)_2$  ( $\text{H}_4\text{L}^2$ ), afforded two novel lead(II) phosphonate–sulfonate hybrids, namely,  $\text{Pb}_3[\text{L}^1][\text{BTS}][\text{H}_2\text{O}] \cdot \text{H}_2\text{O}$  **1** and  $\text{Pb}_2[\text{HL}^3][\text{BTS}] \cdot \text{H}_2\text{O}$  **2** ( $\text{H}_2\text{L}^3 = 3\text{-Pyridyl-CH}_2(\text{Me})\text{N}(\text{CH}_2\text{PO}_3\text{H}_2)$ ).  $\text{H}_2\text{L}^3$  was formed as a result of the decomposition of one phosphonate group in  $\text{H}_4\text{L}^2$  during the reaction. Compound **1** crystallizes in the triclinic space group  $P\bar{1}$  with  $a = 9.9148(4)$  Å,  $b = 10.4382(4)$  Å,  $c = 10.6926(2)$  Å,  $\alpha = 96.495(2)^\circ$ ,  $\beta = 110.599(2)^\circ$ ,  $\gamma = 98.433(2)^\circ$ ,  $V = 1008.31(6)$  Å<sup>3</sup>, and  $Z = 2$ . The structure of compound **1** features a 3D network built from the interconnection of hexanuclear  $\text{Pb}_6(\text{L}^1)_2$  units and 1D double chains of lead(II) carboxylate–sulfonate. Compound **2** crystallizes in the monoclinic space group  $P2_1/c$  with  $a = 9.5403(7)$  Å,  $b = 11.6170(8)$  Å,  $c = 19.7351(15)$  Å,  $\beta = 97.918(2)^\circ$ ,  $V = 2166.4(3)$  Å<sup>3</sup>, and  $Z = 4$ . Compound **2** has a 3D network structure built by the cross-linkage of 1D double chains of lead(II) phosphonates and 2D layers of lead(II) carboxylate–sulfonate.

© 2004 Elsevier Inc. All rights reserved.

**Keywords:** Metal phosphonates; Sulfonates; Hydrothermal synthesis; Open framework; Crystal structures

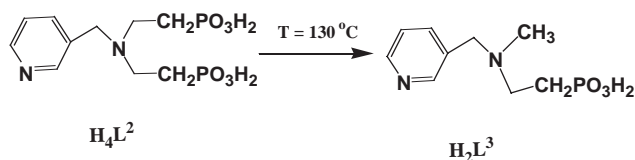
## 1. Introduction

In the past few years, many research efforts have been devoted to the chemistry of metal phosphonates due to their potential applications in the areas of catalysis, ion exchange, proton conductivity, intercalation chemistry, photochemistry, and materials chemistry [1]. Metal phosphonates also exhibit a variety of open frameworks such as layered and open-framework structures. Materials with open-framework structures are promising candidates for hybrid composite materials in electro-optical and sensing applications [2]. In the chemistry of metal phosphonates, the use of bifunctional or multifunctional anionic units, such as diphosphonates, aminophosphonates or phosphonocarboxylates has led to a number of new materials with open-framework structures [3–7]. The strategy of attaching functional groups such as carboxylic

acids, crown ethers and amines to the phosphonic acids has been also proven to be an effective route for the synthesis of metal phosphonates with open-framework architectures [8]. A 3D open-framework tin(II) phosphonopropionate oxalate and a layered tin(II) methylphosphonate oxalate have been reported by the Cheetham group [9a,9b] and a zinc(II) compound of phosphonopropionic acid and 1,3,5-benzene-tricarboxylic acid ( $\text{H}_3\text{BTC}$ ) was isolated; however, the tricarboxylate moiety remains non-coordinated and is also severely disordered [2b]. Two lead(II) compounds of di- or tri-phosphonic acid and  $\text{H}_3\text{BTC}$  have reported in our group, in which the tricarboxylate moiety is involved in metal coordination [9c]. We deem that sulfonic acids should be also capable to form metal sulfonate–phosphonate hybrids. As an expansion of our previous work, we selected one carboxylic-phosphonic acid, *N*-(phosphonomethyl)-*N*-methylglycine,  $\text{MeN}(\text{CH}_2\text{CO}_2\text{H})(\text{CH}_2\text{PO}_3\text{H}_2)$  ( $\text{H}_3\text{L}^1$ ) or a new amino diphosphonic acid, 3-Pyridyl- $\text{CH}_2\text{N}(\text{CH}_2\text{PO}_3\text{H}_2)_2$  ( $\text{H}_4\text{L}^2$ ) and 5-sulfoisophthalic acid monosodium salt ( $\text{NaH}_2\text{BTS}$ )

\*Corresponding author. Fax: +865913714946.

E-mail address: [mjg@ms.fjirsm.ac.cn](mailto:mjg@ms.fjirsm.ac.cn) (J.-G. Mao).



Scheme 1. Formation of  $\text{H}_2\text{L}^3$  by decomposition of  $\text{H}_4\text{L}^2$ .

as the second metal linker. Hydrothermal reactions of the above two phosphonate ligands with lead(II) acetate and  $\text{NaH}_2\text{BTS}$  afforded two novel 3D lead(II) phosphonates, namely,  $\text{Pb}_3[\text{L}^1][\text{BTS}][\text{H}_2\text{O}] \cdot \text{H}_2\text{O}$  **1** and  $\text{Pb}_2[\text{HL}^3][\text{BTS}] \cdot \text{H}_2\text{O}$  **2** ( $\text{H}_2\text{L}^3 = 3\text{-Pyridyl-CH}_2(\text{Me})\text{N}(\text{CH}_2\text{PO}_3\text{H}_2)$ ).  $\text{H}_2\text{L}^3$  was formed as a result of the decomposition of one phosphonate group in  $\text{H}_4\text{L}^2$  under reaction temperature (Scheme 1). Herein, we report their syntheses, characterizations and crystal structures.

## 2. Experimental section

$\text{MeN}(\text{CH}_2\text{CO}_2\text{H})(\text{CH}_2\text{PO}_3\text{H}_2)$  ( $\text{H}_3\text{L}^1$ ), and 3-Pyridyl- $\text{CH}_2\text{N}(\text{CH}_2\text{PO}_3\text{H}_2)_2$  ( $\text{H}_4\text{L}^2$ ) were prepared by a Mannich-type reaction according to procedures described previously [8d,9c,10]. All other chemicals were obtained from commercial sources and used without further purification. Elemental analyses were performed on a Vario EL III elemental analyzer. Thermogravimetric analyses were carried out with a TGA/SBTA851 unit, at a heating rate of  $15^\circ\text{C}/\text{min}$  under a nitrogen atmosphere. IR spectra were recorded on a Magna 750 FT-IR spectrometer photometer as KBr pellets in the  $4000\text{--}400\text{ cm}^{-1}$ . X-ray powder diffraction (XRD) patterns ( $\text{CuK}\alpha$ ) were collected in a sealed glass capillary on a Philips XPERT-MPD diffractometer.

### 2.1. Synthesis of $\text{Pb}_3[\text{L}^1][\text{BTS}][\text{H}_2\text{O}] \cdot \text{H}_2\text{O}$ **1**

Compound **1** was prepared by hydrothermal reaction of lead(II) acetate trihydrate (1.0 mmol, 0.38 g),  $\text{H}_3\text{L}^1$  (1.0 mmol, 0.18 g) and  $\text{NaH}_2\text{BTS}$  (1.0 mmol, 0.26 g) in a 1:1:1 molar ratio in 10.0 mL of deionized water. The mixture was sealed in autoclave equipped with a Teflon liner (25 mL) and then heated at  $130^\circ\text{C}$  for 4 days. The initial and final pH values are 4 and 5, respectively. Colorless crystals of **1** were recovered in a 65.8% yield (based on Pb). Elemental analysis for compound **1**,  $\text{C}_{12}\text{H}_{14}\text{NO}_{14}\text{PSPb}_3$ : C, 13.33%; H, 1.31%; N, 1.30%. Calcd: C, 13.26%; H, 1.14%; N, 1.3%. IR ( $\text{KBr}$ ,  $\text{cm}^{-1}$ ): 3442m, 3068w, 1593s, 1531vs, 1435m, 1394w, 1360vs, 1315w, 1200m, 1115m, 1045m, 997m, 974w, 924w, 779m, 721m, 721m, 673w, 623s, 580w, 519w, 442m.

### 2.2. Synthesis of $\text{Pb}_2[\text{HL}^3][\text{BTS}] \cdot \text{H}_2\text{O}$ **2**

Compound **2** was prepared by hydrothermal reaction of lead(II) acetate trihydrate (0.75 mmol, 0.29 g),  $\text{H}_4\text{L}^2$  (0.25 mmol, 0.08 g) and  $\text{NaH}_2\text{BTS}$  (0.5 mmol, 0.14 g) in a 3:1:2 molar ratio in 10.0 mL of deionized water. The resultant mixture was sealed in an autoclave equipped with a Teflon liner (25 mL) and then heated at  $130^\circ\text{C}$  for 5 days. The pH value of the resultant solution was adjusted to approximately 4 by slow addition of NaOH. Colorless crystals of **2** were recovered in 63.6% yield (based on Pb). Elemental analysis for compound **2**,  $\text{C}_{16}\text{H}_{17}\text{N}_2\text{O}_{11}\text{PSPb}_2$ : C, 21.57%; H, 1.89%; N, 3.14%. Calcd: C, 21.60%; H, 1.81%; N, 3.15%. IR ( $\text{KBr}$ ,  $\text{cm}^{-1}$ ): 3419m, 3059m, 1599s, 1543vs, 1479w, 1431m, 1360vs, 1309w, 1230m, 1196w, 1169w, 1115s, 1082m, 1034s, 960m, 939m, 868w, 845w, 781m, 766w, 723m, 683w, 623m, 567s, 521w, 442w.

### 2.3. Crystallography

Single crystals of **1** and **2** were mounted on a Siemens Smart CCD diffractometer equipped with a graphite-monochromated  $\text{MoK}\alpha$  radiation ( $\lambda = 0.71073 \text{ \AA}$ ). Intensity data were collected by the narrow frame method at 293 K. Both data sets were corrected for Lorentz and polarization as well as for absorption by the SADABS program [11]. Both structures were solved by direct methods and refined by full-matrix least-squares fitting on  $F^2$  by SHELX-97 [11]. All non-hydrogen atoms, except for O(1), C(2), C(14) C(15) and C(17) atoms in **1** and C(3), C(6), C(15) and C(17) atoms in **2**, were refined with anisotropic thermal parameters. All hydrogen atoms except those of the water molecules were located at geometrically calculated positions. Final cycle of refinements reveals featureless residual peak and hole of  $2.62 \text{ e \AA}^{-3}$  ( $1.17 \text{ \AA}$  from O3) and  $-4.07 \text{ e \AA}^{-3}$  ( $0.96 \text{ \AA}$  from Pb3) for compound **1**; and  $1.93 \text{ e \AA}^{-3}$  ( $1.05 \text{ \AA}$  from Pb1) and  $-2.28 \text{ e \AA}^{-3}$  ( $1.19 \text{ \AA}$  from Pb1) for compound **2**, respectively. Crystallographic data and structural refinements are summarized in Table 1. Important bond distances and angles are listed in Table 2.

Crystallographic data (excluding structure factors) for the two structures reported in this paper have been deposited with the Cambridge Crystallographic Data Centre as supplementary publication nos. CCDC 228761 and 228762. Copies of the data can be obtained free of charge on application to CCDC, 12 Union Road, Cambridge CB2 1EZ, UK (fax: (44)-1223-336-033; e-mail: [deposit@ccdc.cam.ac.uk](mailto:deposit@ccdc.cam.ac.uk)).

## 3. Results and discussion

The structure of compound **1** features a complicated 3D network. As shown in Fig. 1, there are three unique

Table 1  
Crystal data and structure refinements for **1** and **2**<sup>a</sup>

Compound	<b>1</b>	<b>2</b>
Formula	C <sub>12</sub> H <sub>14</sub> NO <sub>14</sub> PSPb <sub>3</sub>	C <sub>16</sub> H <sub>17</sub> N <sub>2</sub> O <sub>11</sub> PSPb <sub>2</sub>
<i>F<sub>w</sub></i>	1080.84	890.73
Space group	<i>P</i> $\bar{1}$	<i>P</i> 2 <sub>1</sub> / <i>c</i>
<i>a</i> (Å)	9.9148(4)	9.5403(7)
<i>b</i> (Å)	10.4382(4)	11.6170(8)
<i>c</i> (Å)	10.6926(2)	19.7351(15)
$\alpha$ (deg)	96.495(2)	90.0
$\beta$ (deg)	110.599(2)	97.918(2)
$\gamma$ (deg)	98.433(2)	90.0
<i>V</i> (Å <sup>3</sup> )	1008.31(6)	2166.4(3)
<i>Z</i>	2	4
<i>D</i> <sub>calcd</sub> (g cm <sup>-3</sup> )	3.560	2.731
$\mu$ (mm <sup>-1</sup> ), MoK $\alpha$ (mm <sup>-1</sup> )	25.243	15.756
<i>F</i> (000)	964	1640
Reflections collected	5144	6530
Independent reflections	3477 ( <i>R</i> <sub>int</sub> = 0.0381)	3806 ( <i>R</i> <sub>int</sub> = 0.0608)
Observed reflections	3243	2536
[ <i>I</i> > 2 $\sigma$ ( <i>I</i> )]		
Goodness-of-fit (GOF)	1.096	1.118
<i>R</i> <sub>1</sub> , <i>wR</i> <sub>2</sub> ( <i>I</i> > 2 $\sigma$ ( <i>I</i> )) <sup>a</sup>	0.0408/0.1090	0.0734/0.1270
<i>R</i> <sub>1</sub> , <i>wR</i> <sub>2</sub> (all data)	0.0444/0.1133	0.1288/0.1531

$$^a R_1 = \sum ||F_o| - |F_c|| / \sum |F_o|, wR_2 = \{ \sum w[(F_o)^2 - (F_c)^2]^2 / \sum w(F_o)^2 \}^{1/2}.$$

Pb(II) ions in the asymmetric unit of compound **1**. Pb1 is 5-coordinated by one carboxylate and one phosphonate oxygens from two L<sup>1</sup> ligands, two carboxylate oxygen atoms from a BTS anion and an aqua ligand. Pb2 is 5-coordinated by one carboxylate oxygen atom from one L<sup>1</sup> ligand, three carboxylate oxygen atoms from two BTS anions, and one sulfonate oxygen atom from the third BTS anion. The coordination geometry of Pb1 and Pb2 can be described as a  $\psi$ -PbO<sub>5</sub> octahedron with the lone pair occupying the sixth coordination site. Pb3 is 4-coordinated by a chelating L<sup>1</sup> ligand in a tridentate fashion (O2, N1 and O12), and one phosphonate oxygen O13 from another L<sup>1</sup> ligand. Its coordination geometry can be described as a  $\psi$ -PbO<sub>3</sub>N square pyramid with the lone pair occupying the fifth coordination site. This type of coordination geometry has been reported in other lead phosphonates [9]. The Pb–O distances range from 2.387(8) to 2.721(8) Å, comparable to those reported for other lead(II) phosphonates and lead(II) carboxylates [9,12–14]. The phosphonate ligand anion is heptadentate, it chelates one Pb(II) ion tridentately and bridges four other Pb(II) ions. O2 is bidentate whereas the remaining coordination atoms are unidentate. The BTS<sup>3-</sup> anion is pentadentate. Each carboxylate group chelates with a lead(II) ion bidentately and the sulfonate group is unidentate (O7). O8 and O9 of the sulfonate group remain non-coordinated. Based on charge balance, P–O, S–O and C–O distances as well as their coordination mode, both L<sup>1</sup> and BTS should be 3-, which means that both of them have been deprotonated completely.

Table 2  
Selected bond lengths (Å) and angles (deg) for **1** and **2**

Compound <b>1</b>			
Pb(1)–O(11)#1	2.387(8)	Pb(2)–O(6)#3	2.625(9)
Pb(1)–O(3)#2	2.518(8)	Pb(2)–O(4)#2	2.628(8)
Pb(1)–O(2)	2.639(8)	Pb(2)–O(7)	2.672(10)
Pb(1)–O(1W)	2.694(9)	Pb(3)–O(13)#1	2.359(7)
Pb(1)–O(4)#2	2.721(8)	Pb(3)–O(12)	2.363(8)
Pb(2)–O(1)	2.415(9)	Pb(3)–O(2)	2.554(8)
Pb(2)–O(5)#3	2.463(9)	Pb(3)–N(1)	2.637(9)
O(11)#1–Pb(1)–O(3)#2	72.5(3)	O(1)–Pb(2)–O(6)#3	120.6(3)
O(11)#1–Pb(1)–O(2)	81.8(3)	O(5)#3–Pb(2)–O(6)#3	50.6(3)
O(3)#2–Pb(1)–O(2)	145.5(3)	O(1)–Pb(2)–O(4)#2	76.5(3)
O(11)#1–Pb(1)–O(1W)	74.0(3)	O(5)#3–Pb(2)–O(4)#2	82.4(3)
O(3)#2–Pb(1)–O(1W)	84.0(3)	O(6)#3–Pb(2)–O(4)#2	83.5(3)
O(2)–Pb(1)–O(1W)	110.9(3)	O(1)–Pb(2)–O(7)	89.6(3)
O(11)#1–Pb(1)–O(4)#2	71.2(3)	O(5)#3–Pb(2)–O(7)	92.6(4)
O(3)#2–Pb(1)–O(4)#2	49.7(2)	O(6)#3–Pb(2)–O(7)	103.5(3)
O(2)–Pb(1)–O(4)#2	100.7(2)	O(4)#2–Pb(2)–O(7)	166.1(3)
O(1W)–Pb(1)–O(4)#2	128.2(3)	O(13)#1–Pb(3)–O(12)	80.4(3)
O(1)–Pb(2)–O(5)#3	71.5(3)	O(13)#1–Pb(3)–O(2)	73.1(3)
O(13)#1–Pb(3)–N(1)	114.2(3)	O(12)–Pb(3)–O(2)	111.3(3)
O(2)–Pb(3)–N(1)	72.1(3)	O(2)–Pb(3)–N(1)	64.2(3)
O(11)#1–Pb(1)–O(3)#2	72.5(3)	O(1)–Pb(2)–O(6)#3	120.6(3)
O(11)#1–Pb(1)–O(2)	81.8(3)	O(5)#3–Pb(2)–O(6)#3	50.6(3)
O(3)#2–Pb(1)–O(2)	145.5(3)	O(1)–Pb(2)–O(4)#2	76.5(3)
Compound <b>2</b>			
Pb(1)–O(12)	2.318(16)	Pb(2)–O(4)	2.619(19)
Pb(1)–O(2)	2.537(16)	Pb(2)–O(13)#4	2.358(15)
Pb(1)–N(2)#1	2.61(2)	Pb(2)–O(11)#5	2.375(14)
Pb(1)–O(4)#2	2.705(16)	Pb(2)–O(3)	2.498(18)
Pb(1)–O(13)#3	2.731(16)	Pb(2)–O(21)#6	2.769(19)
Pb(1)–O(1)	2.785(17)		
O(12)–Pb(1)–O(2)	76.8(5)	N(2)#1–Pb(1)–O(13)#3	147.5(6)
O(12)–Pb(1)–N(2)#1	76.7(6)	O(4)#2–Pb(1)–O(13)#3	113.1(5)
O(2)–Pb(1)–N(2)#1	80.0(6)	O(13)#4–Pb(2)–O(11)#5	83.8(5)
O(12)–Pb(1)–O(4)#2	77.9(6)	O(13)#4–Pb(2)–O(3)	95.0(7)
O(2)–Pb(1)–O(4)#2	153.6(6)	O(11)#5–Pb(2)–O(3)	120.2(6)
N(2)#1–Pb(1)–O(4)#2	87.2(6)	O(13)#4–Pb(2)–O(4)	99.8(6)
O(12)–Pb(1)–O(13)#3	82.9(5)	O(11)#5–Pb(2)–O(4)	70.2(5)
O(2)–Pb(1)–O(13)#3	70.8(5)		

Symmetry transformations used to generate equivalent atoms: For **1**: #1  $-x + 1, -y + 2, -z + 1$ ; #2  $x, y, z + 1$ ; #3  $-x + 2, -y + 1, -z + 1$ ; #4  $x, y, z - 1$ . For **2**: #1  $x - 1, y, z$ ; #2  $x, -y + 1/2, z - 1/2$ ; #3  $-x + 1, -y + 1, -z + 1$ ; #4  $x, -y + 1/2, z + 1/2$ ; #5  $-x + 1, y - 1/2, -z + 3/2$ ; #6  $-x, y - 1/2, -z + 3/2$ .

The interconnection of the Pb(II) ions via chelating and bridging L<sup>1</sup> ligands leads to the formation of Pb<sub>6</sub>(L<sup>1</sup>)<sub>2</sub> unit (Fig. 2a), whereas the interconnection of the Pb(II) ions via bridging BTS anions resulted in a 1D double chain along the *c*-axis (Fig. 2b). The cross-linkage of the above two building blocks leads to a complicated 3D network (Fig. 3). The lattice water molecule is located in the cavity of the structure, it is hydrogen bonded to the aqua ligand (O(1w)⋯O(2w) 2.748(14) Å).

Compound **2** was obtained by hydrothermal reaction of lead(II) acetate with NaH<sub>2</sub>BTS and the aminodiphosphonic acid, 3-pyridyl-CH<sub>2</sub>NH(CH<sub>2</sub>PO<sub>3</sub>H<sub>2</sub>)<sub>2</sub> (H<sub>4</sub>L<sup>2</sup>). During the reaction, one phosphonate group of H<sub>4</sub>L<sup>2</sup>

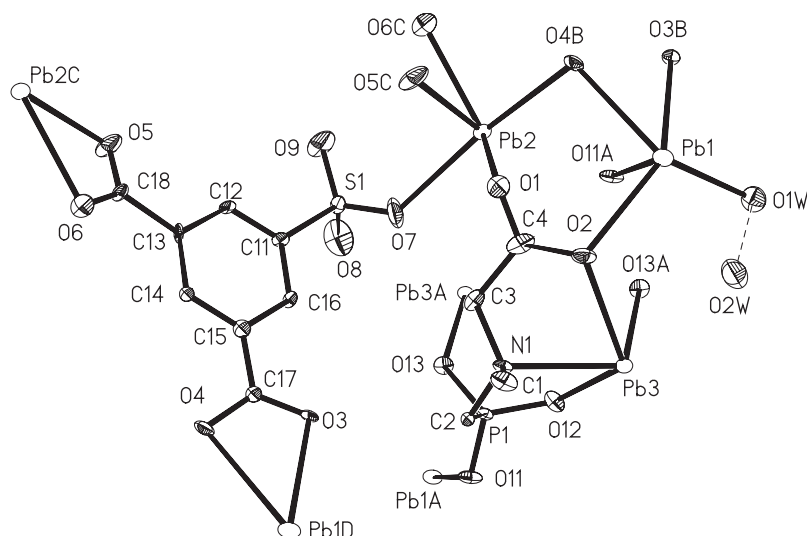


Fig. 1. ORTEP representation of the selected unit of compound **1**. The thermal ellipsoids are drawn at 50% probability. The dotted line represents the hydrogen bond.

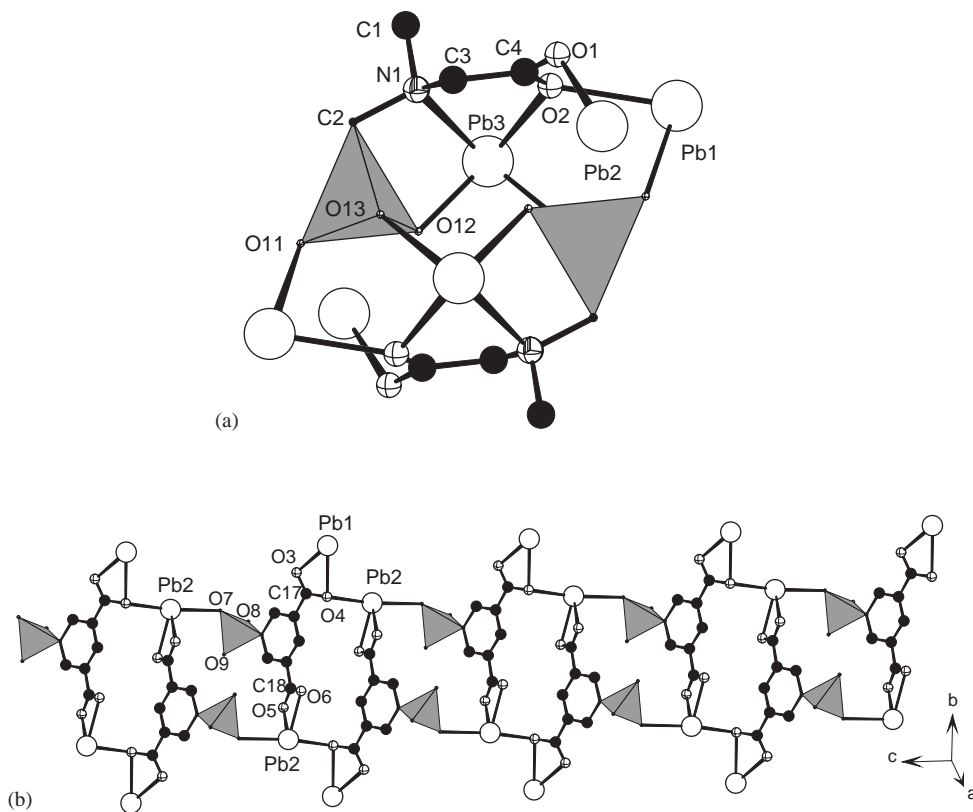


Fig. 2. (a) A  $\text{Pb}_6(\text{L}^1)_2$  hexanuclear phosphonate unit; (b) A 1D double chain of lead(II) carboxylate-sulfonate in compound **1**. The  $\text{CSO}_3$  and  $\text{CPO}_3$  tetrahedra are shaded in gray. Pb, C, O and N atoms are drawn as open, black, crossed and octanded circles, respectively.

was decomposed to give a new monophosphonate ligand  $\text{H}_2\text{L}^3$ . The structure of **2** features a 3D network. As shown in Fig. 4, there are two unique Pb(II) ions in the asymmetric unit of compound **2**. Pb1 is 6-coordinated by two phosphonate oxygens and one pyridyl nitrogen atom of three  $\text{HL}^3$  ligands, as well as

three carboxylate oxygens from two  $\text{BTS}^-$  anions. Pb2 is 5-coordinated by two phosphonate oxygens of two  $\text{HL}^3$  ligands, and two carboxylate oxygens and one sulfonate oxygen from two  $\text{BTS}^-$  anions. The Pb1 has a  $\psi\text{-PbO}_5$  octahedral geometry in which the sixth coordination site is occupied by the lone pair electrons. The coordination

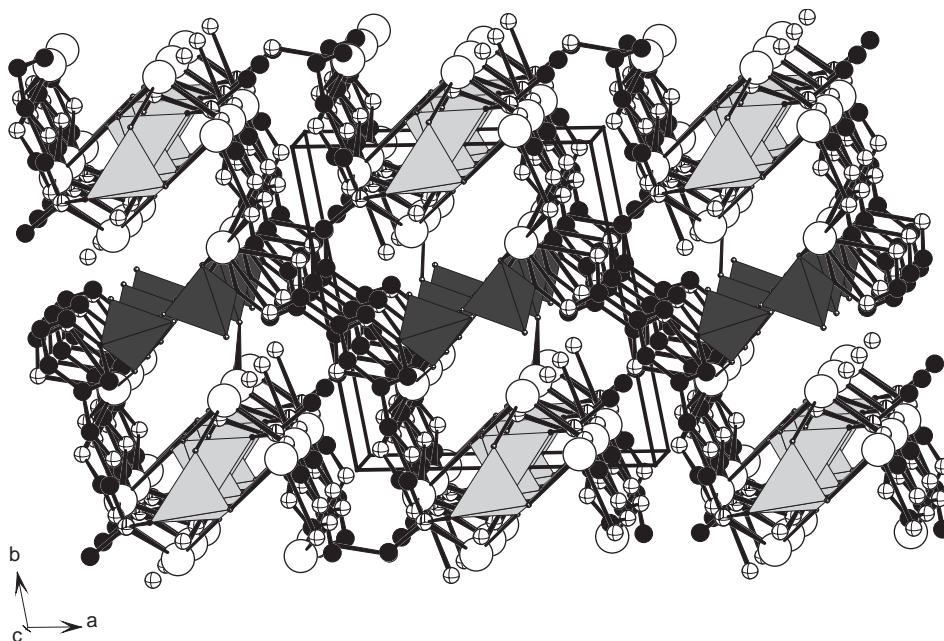


Fig. 3. View of the structure of **1** down the  $c$ -axis. The  $\text{CSO}_3$  and  $\text{CPO}_3$  tetrahedra are shaded in dark and light gray, respectively. Pb, C, O and N atoms are drawn as open, black, crossed and octanded circles, respectively.

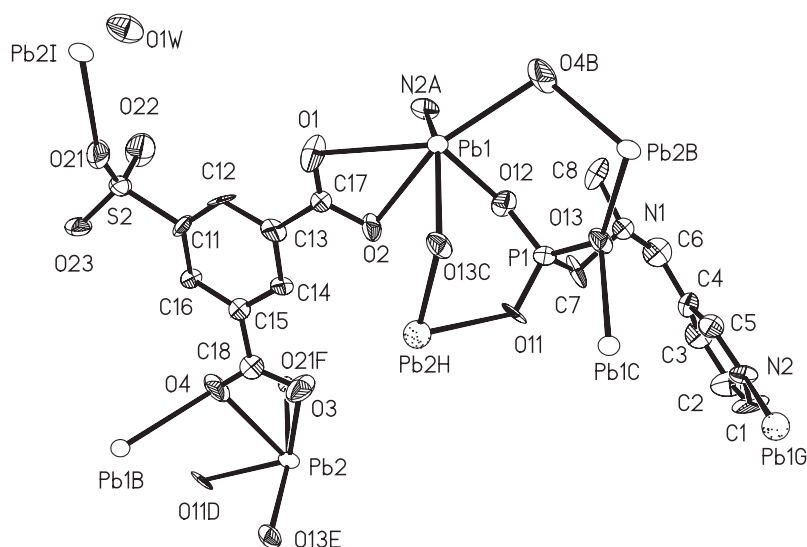


Fig. 4. ORTEP representation of the selected unit of compound **2**. The thermal ellipsoids are drawn at 50% probability.

geometry of Pb2 is a severely distorted  $\text{PbO}_5\text{N}$  octahedron, the distortion was caused by the lone pair electrons. The Pb–O distances range from 2.318(16) to 2.785(17) Å, which are comparable to those in **1** and other lead(II) phosphonates [9,12–14].

Based on the requirement of charge balance as well as P–O, C–O and S–O distances, the  $\text{HL}^3$  phosphonate anion is  $-1$  and the sulfonate-carboxylate BTS ligand is  $-3$  in charge. The amino group N1 of the phosphonate ligand is protonated. The phosphonate anion is pentadentate and bridges with five Pb(II) ions. O13 of the phosphonate group is  $\mu_2$ -bridging, whereas O11 and

O12 are unidentate. It is interesting to note that the pyridyl N atom is also involved in the metal coordination. The  $\text{BTS}^{3-}$  anion is hexadentate and bridges with four Pb(II) ions. One carboxylate group (O1–C17–O2) is bidentate chelating, whereas the other one composed of O3–C18–O4 is  $\mu_3$  chelating and bridging. The sulfonate BTS ligand is unidentate (O21). O22 and O23 remain non-coordinated.

The interconnection of Pb1 and Pb2 atoms by the phosphonate groups resulted in a  $\text{Pb}_4(\text{HL}^3)_2$  unit, and such neighboring units are bridged by the pyridine groups to form a 1D double chain along the  $a$ -axis

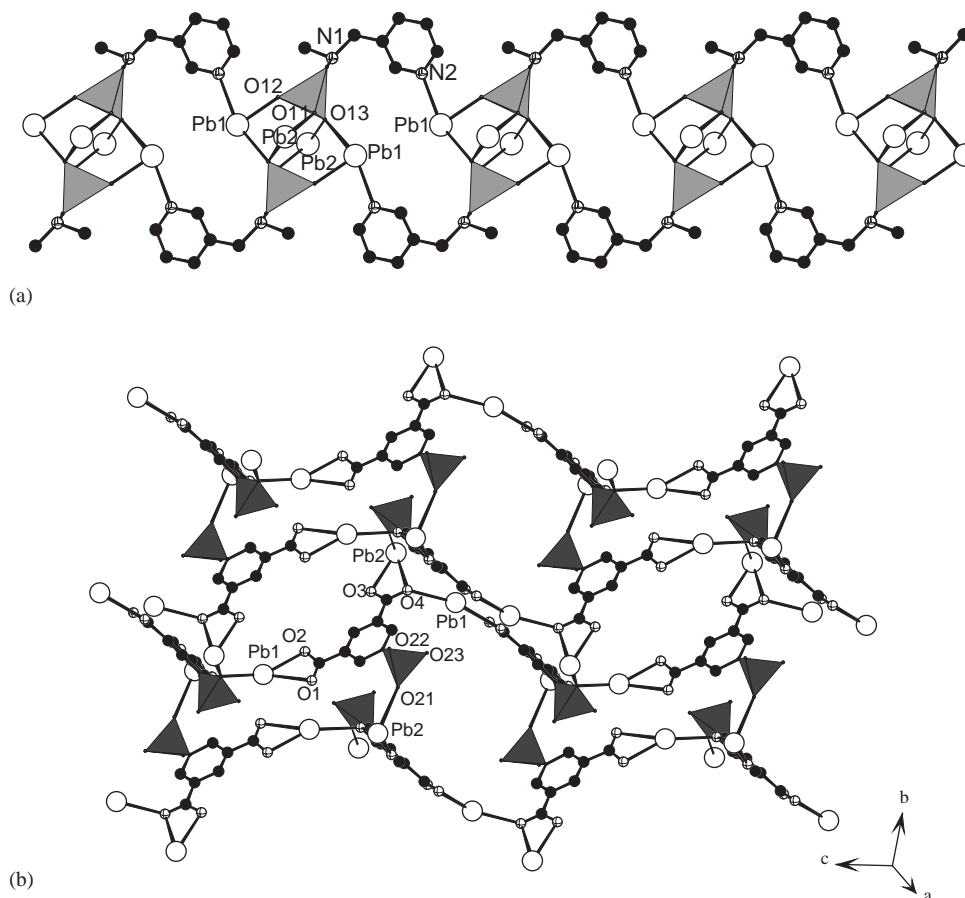


Fig. 5. (a) A 1D double chain of lead(II) phosphonate; (b) A 2D layer of lead(II) carboxylate-sulfonate in compound **2**. The  $\text{CSO}_3$  and  $\text{CPO}_3$  tetrahedra are shaded in dark and light gray, respectively. Pb, C, O and N atoms are drawn as open, black, crossed and octaded circles, respectively.

(Fig. 5a). The interconnection of the Pb(II) ions by bridging and chelating BTS anions leads to a 2D layer (Fig. 5b). The cross-linkage of the above two building units resulted in a 3D network with large cavities (Fig. 6). The size of the cavity is estimated to be  $12.0 \times 16.0 \text{ \AA}^2$  based on crystal structure. The pyridyl rings and two water molecules are located at these micropores. The lattice water molecule O1W is hydrogen bonded with the non-coordinated sulfonate oxygen O22 with an O...O separation of  $2.914(20) \text{ \AA}$ . The protonated N1 atom forms a hydrogen bond with the other non-coordination sulfonate oxygen (O23). The N1...O23 (symmetry code:  $x + 1, 1/2 - y, -1/2 + z$ ) separation is  $2.912(25) \text{ \AA}$ .

The XRD powder patterns for compounds **1** and **2** were collected on a Philips X'Pert-MPD diffractometer using graphite-monochromated  $\text{CuK}\alpha$  radiation in the angular range of  $2\theta = 5 - 70^\circ$ . The measured powder patterns match with the ones simulated from their single crystal structure data, thus both compounds were obtained as a single phase.

The IR spectra of both compounds **1** and **2** were measured. The broadband at  $3442$  and  $3068 \text{ cm}^{-1}$  for compound **1** can be assigned to the O-H stretching vibrations, such bands appeared at  $3419$  and  $3059 \text{ cm}^{-1}$

for compound **2**. The asymmetric vibration absorption band of the sulfonate group appeared at  $1200 \text{ cm}^{-1}$  in compound **1** and at  $1196 \text{ cm}^{-1}$  in compound **2**. Absorption band around  $623 \text{ cm}^{-1}$  is characteristic band for  $\nu_{\text{S-O}}$  of the sulfonate group. The two strong bands at  $1593$  and  $1531 \text{ cm}^{-1}$  for compound **1** or  $1599$  and  $1543 \text{ cm}^{-1}$  for compound **2** correspond to the antisymmetric stretching bands of the carboxylate groups. The symmetric stretching bands of the carboxylate group appeared around  $1435$  and  $1431 \text{ cm}^{-1}$ , respectively for compounds **1** and **2**. The bands from  $900$ – $1100 \text{ cm}^{-1}$  are due to the stretching vibrations of the tetrahedral  $\text{CPO}_3$  group.

The TGA diagram of **1** shows three main steps of the weight losses (Fig. 7). The first step is loss of one lattice water molecules, which started at  $78^\circ\text{C}$  and was completed at  $243^\circ\text{C}$ , the observed weight loss of  $1.68\%$  is in good agreement with the calculated value ( $1.69\%$ ). The second step covering a temperature range of  $356$ – $530^\circ\text{C}$  corresponds to the burning of BTS and phosphonate ligands. The third step overlapped with the second one and continued up to  $1000^\circ\text{C}$ , during which the compound was further decomposed. The final product is a mixture of  $\text{Pb}_2\text{P}_2\text{O}_7$  and  $\text{PbO}$  based on

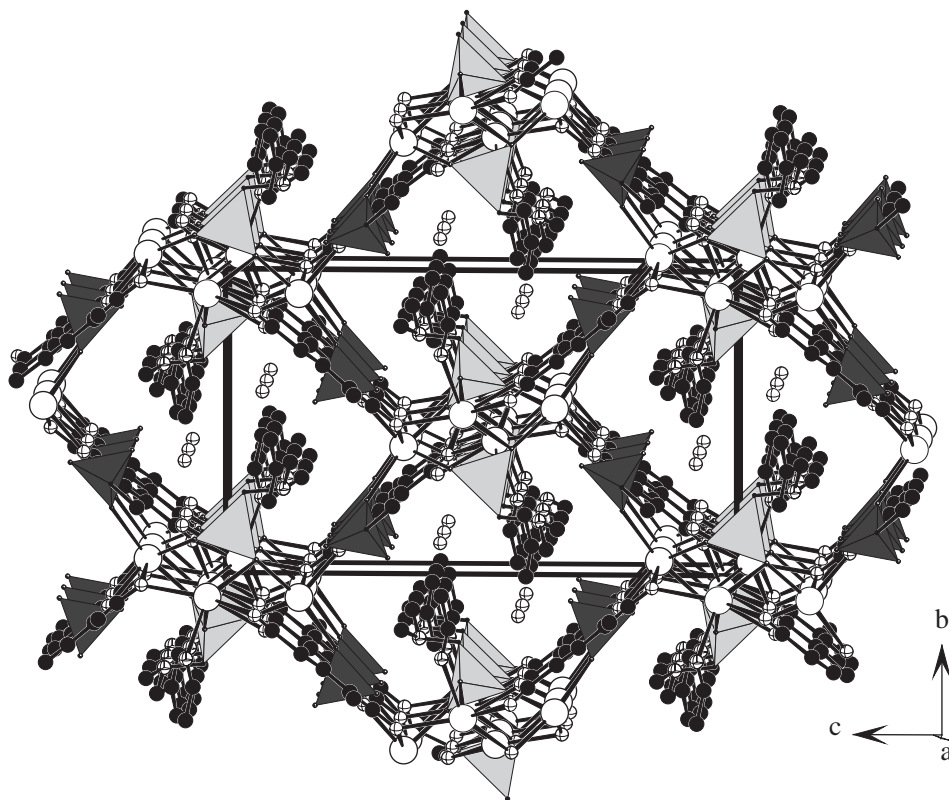


Fig. 6. View of the structure of compound **2** down the *a*-axis. The  $\text{CSO}_3$  and  $\text{CPO}_3$  tetrahedra are shaded in dark and light gray, respectively. Pb, C, O and N atoms are drawn as open, black, crossed and octahedrons, respectively.

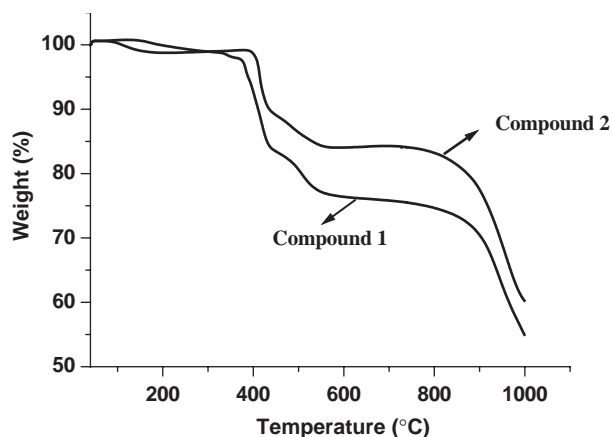


Fig. 7. TGA curves of compounds **1** and **2**.

the XRD powder diffraction. The total weight loss is 45.0%. The TGA curves of **2** exhibit also three steps of weight losses (Fig. 7). The first step is release of the partial lattice water molecules, which started at 92°C and was completed at 295°C, the observed weight loss of 1.3% is slightly less than the theoretical one (2.02%). The second weight loss starting at 392°C and continued up to 550°C, which corresponds to the burning of BTS and phosphonate ligands. The third step covers a temperature range of 760–1000°C, corresponding to the further decomposition of the compound. The final product is a mixture of PbO and  $\text{Pb}_2\text{P}_2\text{O}_7$  based on

XRD powder diffraction. The total weight loss is of 40.1% (Fig. 7).

### Acknowledgments

This work was supported by the National Natural Science Foundation of China (20371047).

### References

- [1] (a) E.W. Stein Sr, A. Clearfield, M.A. Subramanian, *Solid State Ionics* 83 (1996) 113;
  - (b) G. Alberti, U. Costantino, in: J.M. Lehn (Ed.), *Comprehensive Supramolecular Chemistry*, Pergamon-Elsevier Science Ltd., London, 1996, p. 1;
    - (c) A. Clearfield, *Curr. Opin. Solid State Mater. Sci.* 1 (1996) 268;
      - (d) A. Clearfield, in: K.D. Karlin (Ed.), *Metal Phosphonate Chemistry in Progress in Inorganic Chemistry*, Vol. 47, Wiley, New York, 1998, pp. 371–510 (and references therein).
  - [2] (a) A.K. Cheetham, G. Ferey, T. Loiseau, *Angew. Chem. Int. Ed.* 38 (1999) 3269;
    - (b) J. Zhu, X. Bu, P. Feng, G.D. Stucky, *J. Am. Chem. Soc.* 122 (2000) 11563.
  - [3] (a) N.L. Rosi, M. Eddaoudi, J. Kim, M. O’Keeffe, O.M. Yaghi, *Angew. Chem. Int. Ed.* 41 (2001) 284;
    - (b) M. Eddaoudi, J. Kim, M. O’Keeffe, O.M. Yaghi, *J. Am. Chem. Soc.* 124 (2002) 376;
      - (c) M.E. Braun, C.D. Steffek, J. Kim, P.G. Rasmussen, O.M. Yaghi, *Chem. Commun.* (2001) 2532.

- [4] (a) A. Distler, L. Lohse, S.C. Sevov, J. Chem. Soc., Dalton Trans. (1999) 1805;  
(b) V. Soghomonian, Q. Chen, R.C. Haushalter, J. Zubieta, Angew. Chem. Int. Ed. 34 (1995) 223.
- [5] (a) S. Drumel, P. Janvier, D. Deniaud, B. Bujoli, J. Chem. Soc., Chem. Commun. (1995) 1051;  
(b) U. Costantino, M. Nocchetti, R. Vivani, J. Am. Chem. Soc. 124 (2002) 8428;  
(c) S.O.H. Gutschke, D.J. Price, A.K. Powell, P.T. Wood, Angew. Chem. Int. Ed. 38 (1999) 1088;  
(d) E. Galdecka, Z. Galdecki, P. Gawryszewska, J. Legendziewicz, New J. Chem. 24 (2000) 387;  
(e) L.-M. Zheng, P. Yin, X.-Q. Xin, Inorg. Chem. 41 (2002) 4084.
- [6] (a) N. Stock, S.A. Frey, G.D. Stucky, A.K. Cheetham, J. Chem. Soc., Dalton Trans. (2000) 4292;  
(b) S. Ayyappan, G.D. Delgado, A.K. Cheetham, G. Férey, C.N.R. Rao, J. Chem. Soc., Dalton Trans. (1999) 2905;  
(c) F. Fredoueil, M. Evain, D. Massiot, M. Bujoli-Doeuff, P. Janvier, A. Clearfield, B. Bujoli, J. Chem. Soc., Dalton Trans. (2002) 1508;  
(d) S. Drumel, M. Bujolidoeuff, P. Janvier, B. Bujoli, New J. Chem. 19 (1995) 239.
- [7] (a) M. Riou-Cavellec, M. Sanselme, M. Nogues, J.M. Greneche, G. Férey, Solid State Sci. 4 (2002) 619;  
(b) M. Sanselme, M. Riou-Cavellec, J.M. Greneche, G. Férey, J. Solid State Chem. 164 (2002) 354;  
(c) M. Riou-Cavellec, M. Sanselme, N. Guillou, G. Férey, Inorg. Chem. 40 (2001) 723;  
(d) M. Riou-Cavellec, M. Sanselme, G. Férey, J. Mater. Chem. 10 (2000) 745.
- [8] (a) J.-G. Mao, Z. Wang, A. Clearfield, Inorg. Chem. 41 (2002) 2334;  
(b) J.-G. Mao, Z. Wang, A. Clearfield, J. Chem. Soc., Dalton Trans. (2002) 4541;  
(c) J.-G. Mao, Z. Wang, A. Clearfield, Inorg. Chem. 41 (2002) 3713;  
(d) C. Lei, J.-G. Mao, Y.-Q. Sun, H.-Y. Zeng, A. Clearfield, Inorg. Chem. 42 (2003) 6157.
- [9] (a) N. Stock, G.D. Stucky, A.K. Cheetham, Chem. Commun. (2000) 2277;  
(b) B. Adair, S. Natarajan, A.K. Cheetham, J. Mater. Chem. 8 (1998) 1477;  
(c) J.-L. Song, J.-G. Mao, Y.-Q. Sun, A. Clearfield, Eur. J. Inorg. Chem. (2003) 4218.
- [10] (a) J.-G. Mao, Z. Wang, A. Clearfield, New J. Chem. 26 (2002) 1010;  
(b) M. Galanski, B.K. Keppler, B. Nuber, Angew. Chem., Int. Ed. 34 (1995) 1103.
- [11] (a) G.M. Sheldrick, SADABS, Universität Göttingen, 1995;  
(b) G.M. Sheldrick, SHELXTL, Crystallographic Software Package, version 5.1, Bruker-AXS, Madison, WI, 1998.
- [12] (a) E. Irran, T. Bein, N. Stock, J. Solid State Chem. 173 (2003) 293;  
(b) N. Stock, N. Guillou, T. Bein, G. Férey, Solid State Sci. 5 (2003) 629;  
(c) N. Stock, Solid State Sci. 4 (2002) 1089;  
(d) Z.-M. Sun, J.-G. Mao, Y.-Q. Sun, A. Clearfield, New J. Chem. 27 (2003) 1326.
- [13] (a) A. Cabeza, M.A.G. Aranda, S. Bruque, A. Clearfield, J. Mater. Chem. 9 (1999) 571;  
(b) C.V.K. Sharma, A. Clearfield, A. Cabeza, M.A.G. Aranda, S. Bruque, J. Am. Chem. Soc. 123 (2001) 2885;  
(c) A. Cabeza, O.Y. Xiang, C.V.K. Sharma, M.A.G. Aranda, S. Bruque, A. Clearfield, Inorg. Chem. 41 (2002) 2325.
- [14] M.R.St.J. Foreman, T. Gelbrich, M.B. Hursthouse, M.J. Plater, Inorg. Chem. Commun. 3 (2000) 234.